

Lowest-order predictions
for the processes $\gamma\gamma \rightarrow 4f$ and $\gamma\gamma \rightarrow 4f + \gamma^\dagger$

Markus Roth
Max-Planck-Institut, Munich

September 2, 2004

in collaboration with Axel Bredenstein and Stefan Dittmaier

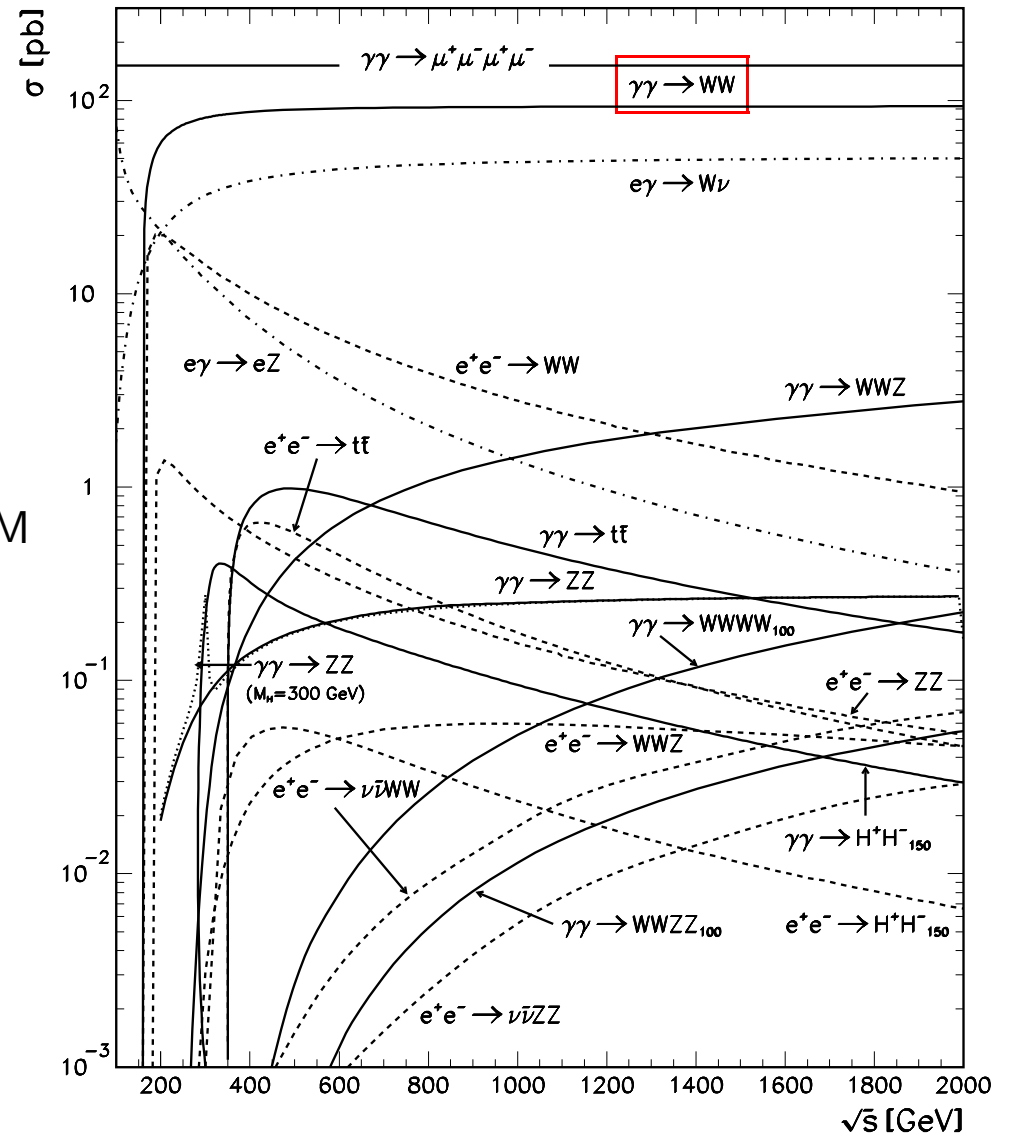
[†]based on the results of Eur. Phys. J. C **36** (2004) 341 (hep-ph/0405169)

Introduction

Baillargeon, et al.'95

Motivation for $\gamma\gamma \rightarrow 4f(+\gamma)$

- One of the **largest** cross sections
 $\gamma\gamma \rightarrow WW \rightarrow 4f$ is **precision observable**
 \Rightarrow Radiative corrections important!
 (Possibility for detector calibration?)
- **Triple- and quartic-gauge-boson couplings**
 \Rightarrow Precision test of the gauge sector of the SM
 $\gamma\gamma \rightarrow WW$ sensitive to $\gamma WW, \gamma\gamma WW$
 $e^+e^- \rightarrow WW$ sensitive to $\gamma WW, ZWW$
- Loop-induced **Higgs production** $\gamma\gamma \rightarrow H$,
 (similar to $gg \rightarrow H$ at the LHC)
 \Rightarrow One of the most important Higgs-
 production channels



Theoretical status

Existing numerical studies for $\gamma\gamma \rightarrow 4f$

- Moretti'97
- Boos, Ohl'97
- Baillargeon, Bélanger, Boudjema'97

⇒ Monochromatic photon beams, only leptonic and semi-leptonic final states

Multi-purpose event generators

- GRACE
- PHEGAS & HELAC
- WHIZARD & MADGRAPH/O'MEGA

Ishikawa et al.'92

Papadopoulos, Kanaki'00

Kilian'01; Stelzer, Long'94; Moretti et al.'01

Dedicated Monte Carlo generator for $\gamma\gamma \rightarrow 4f(+\gamma)$

- Bredenstein, Dittmaier, M.R.'04 ⇒ this work
 - Detailed numerical study for lowest-order processes $\gamma\gamma \rightarrow 4f$ and $\gamma\gamma \rightarrow 4f + \gamma$
 - First step in the calculation of radiative corrections for $\gamma\gamma \rightarrow WW \rightarrow 4f$

Details of the calculation

Features of the calculation

- Monte Carlo event generator for $\gamma\gamma \rightarrow 4f$ and $\gamma\gamma \rightarrow 4f + \gamma$
- **All** $4f(+\gamma)$ final states, full lowest-order amplitudes (including gluon-exchange diagrams)
- All fermions massless
- **Multi-channel integration technique** with adaptive optimization
- **Realistic photon spectrum** implemented in the parameterization of COMPAZ

Zarnecki'02; Telnov'95;
Chen et al.'95

Main complications for $\gamma\gamma \rightarrow 4f(+\gamma)$

- **Fast evaluation** of diagrams with complicated structure due to 2(3) external photon lines

Number of diagrams:	6(24)	$\nu_e \bar{\nu}_e u \bar{u}(\gamma)$
(unitary gauge, no gluons)	:	
	71(468)	$u \bar{u} d \bar{d}(\gamma)$

- **Rich peaking structure**
 \Rightarrow many different channels (=8-dim. phase space), one channel for each diagram
- **Stable numerical convolution** over the photon spectra
- **Gauge invariance** in presence of unstable particles

Generic calculation of amplitudes

- Analytic part: **helicity amplitudes for generic diagrams**

Evaluation with **Weyl–van der Waerden spinors** and use of discrete symmetries

$\gamma\gamma \rightarrow 4f$: 2 compact functions for 1 generic diagram,
for all final states and polarizations

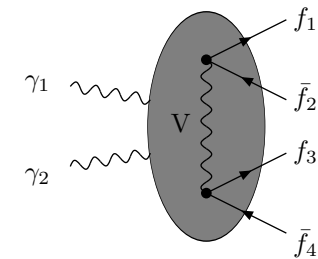
$\gamma\gamma \rightarrow 4f\gamma$: Fortran code for each generic diagram
generated by a Mathematica program

- Combinatorics: **field insertions for generic diagrams**

Permutations of external fermions and insertions of internal fermion and boson fields

- Square amplitude: **squared diagrams and interferences**

Fermi signs and colour algebra (for gluon-exchange diagrams)



Simplification from non-linear gauge fixing

$$\mathcal{L}_{\text{fix},W} = - \left| \partial^\mu W_\mu^+ - iM_W \phi^+ + ie \left(A^\mu - \frac{c_W}{s_W} Z^\mu \right) W_\mu^+ \right|^2.$$

\Rightarrow No $\gamma\phi W$ coupling and simplified VWW , γVWW vertices ($V = \gamma, Z$)

Introduction of decay widths

Optional: constant, step, running width, complex-mass scheme

⇒ Important for controlling gauge invariance

- **Gauge invariant** complex-mass scheme: replace everywhere as well as $\cos^2 \theta_w \rightarrow \frac{M_W^2 - i\Gamma_W M_W}{M_Z^2 - i\Gamma_Z M_Z}$.
Denner, Dittmaier, M.R., Wackerth'99

Numerical integration

- **Multi-channel Monte Carlo integration**

A channel corresponds to each diagram, importance sampling for all propagators
(6–468 different channels)

Berends, Daverveldt, Kleiss'85
Hilgart, Kleiss, Le Diberder'93

- **Adaptive weight optimization**

Kleiss, Pittau '94

- Phase-space generators similar to RACOONWW and LUSIFER

Denner, Dittmaier, M.R., Wackerth'00, '01
Dittmaier, M.R. '02

Compact phase-space generator for each generic diagram

- Standard cut already taken into account in event generation:
invariant-mass cuts, energy cuts, angular cuts

⇒ Important for the numerical stability and efficiency

Implementation of the photon spectra

$$d\sigma = \int_0^1 dx_1 \int_0^1 dx_2 f_\gamma(x_1) f_\gamma(x_2) d\sigma_{\gamma\gamma}(x_1 P_1, x_2 P_2).$$

- **Importance sampling** in numerical integration over the photon spectra $f_\gamma(x)$

Method:

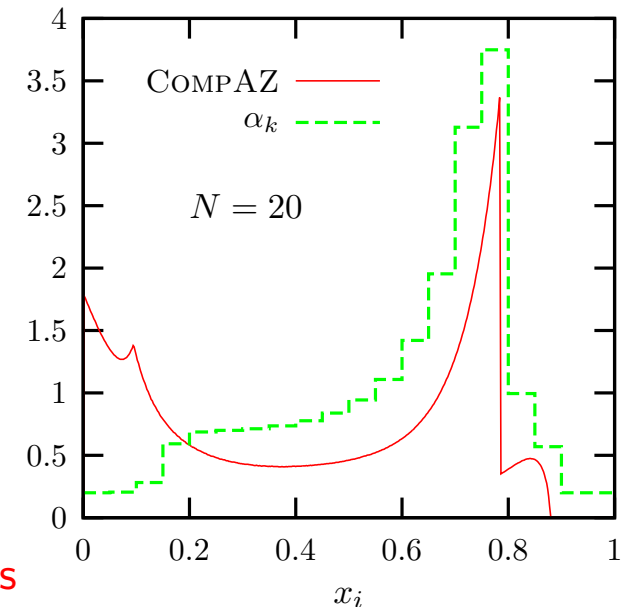
- decompose x -range in N equal bins ($N = 500$)
- choose a bin with probability α_k
- divide weight by α_k ($\sum_k \alpha_k = 1$)

Choose $\alpha_k \propto$ cross section in bin i

Polarization of the laser beam: -1

Polarization of the electron beam: $+0.85$

$f_\gamma(x_i), \alpha_k \times N$



- Photon spectra determine the **polarization of the incoming photons**

Process	σ_{4f} [fb]	$\sigma_{4f\gamma}$ [fb]
$\gamma\gamma \rightarrow e^- \bar{\nu}_e u \bar{d}(\gamma)$	565.05(33)	14.216(27)
$\gamma\gamma \rightarrow \nu_e e^+ d \bar{u}(\gamma)$	558.39(32)	15.459(30)

\Rightarrow Cross sections for CP-equivalent final states are not equal!

Comparison with MADGRAPH & WHIZARD

Outcome of comparison with MADGRAPH & WHIZARD:

- **Very good agreement** between our results and the results of MADGRAPH & WHIZARD
- Statistical errors are comparable
- MADGRAPH & WHIZARD **up to 10 times slower** for complicated neutral-current processes

Without photon spectrum

With photon spectrum

$\gamma\gamma \rightarrow$	$(\sigma - \sigma_W)/\sqrt{\Delta\sigma^2 + \Delta\sigma_W^2}$				$\Delta\sigma_W/\Delta\sigma$	$(\sigma - \sigma_W)/\sqrt{\Delta\sigma^2 + \Delta\sigma_W^2}$				$\Delta\sigma_W/\Delta\sigma$
	-2σ	-1σ	1σ	2σ		-2σ	-1σ	1σ	2σ	
$e^- \bar{\nu}_e \nu_\mu \mu^-$					1.24					1.58
$e^- e^+ \nu_\mu \bar{\nu}_\mu$					1.26					1.73
$e^- e^+ \mu^- \mu^-$					0.64					0.82
$e^- e^+ e^- e^+$					0.62					0.78
$e^- e^+ \nu_e \bar{\nu}_e$					1.26					1.62
$e^- \bar{\nu}_e u \bar{d}$					1.24					1.55
$\nu_e e^+ d \bar{u}$					1.24					1.54
$\nu_e \bar{\nu}_e u \bar{u}$					1.14					1.40
$\nu_e \bar{\nu}_e d \bar{d}$					1.08					1.27
$e^- e^+ u \bar{u}$					0.69					0.80
$e^- e^+ d \bar{d}$					0.95					1.19
$u \bar{d} s \bar{c}$					1.22					1.48
$u \bar{u} c \bar{c}$					0.63					0.82
$u \bar{u} s \bar{s}$					0.97					1.26
$d \bar{d} s \bar{s}$					1.03					1.30
$u \bar{u} u \bar{u}$					0.65					0.93
$d \bar{d} d \bar{d}$					1.13					1.35
$u \bar{u} d \bar{d}$					1.21					1.52

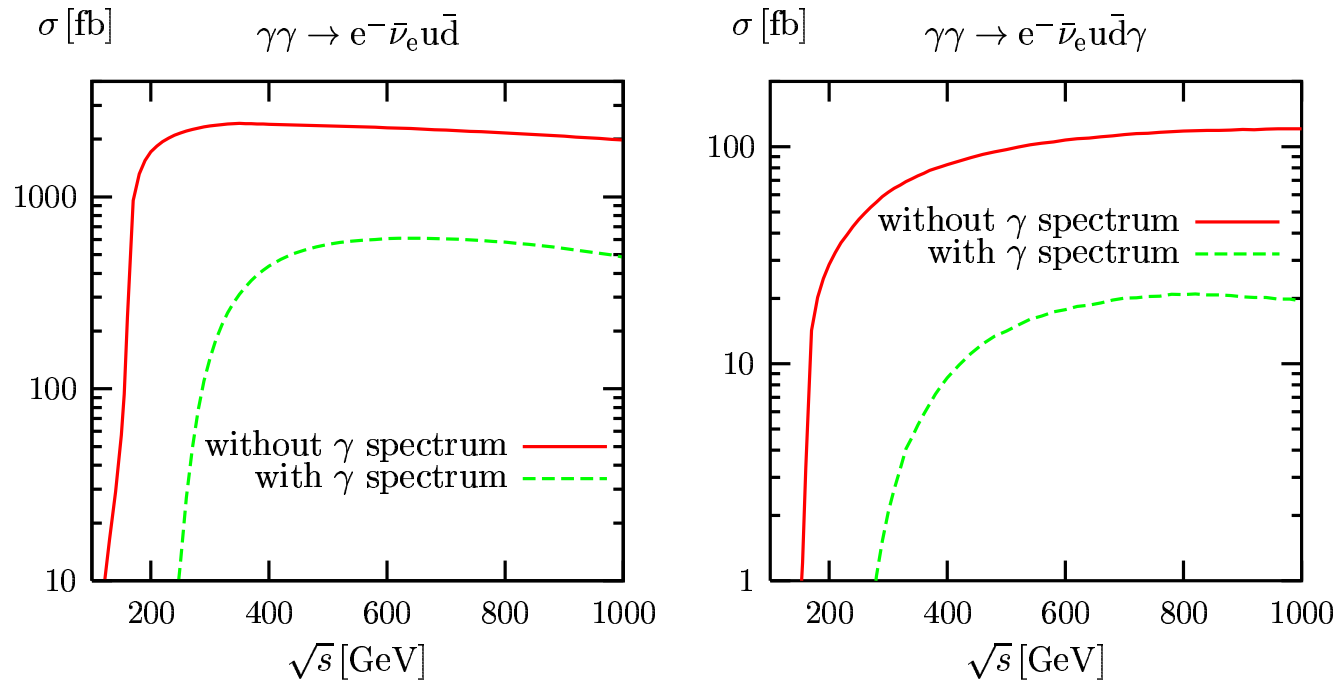
Without photon spectrum

With photon spectrum

$\gamma\gamma \rightarrow$	$(\sigma - \sigma_W)/\sqrt{\Delta\sigma^2 + \Delta\sigma_W^2}$				$\Delta\sigma_W/\Delta\sigma$	$(\sigma - \sigma_W)/\sqrt{\Delta\sigma^2 + \Delta\sigma_W^2}$				$\Delta\sigma_W/\Delta\sigma$
	-2σ	-1σ	1σ	2σ		-2σ	-1σ	1σ	2σ	
$e^- \bar{\nu}_e \nu_\mu \mu^- \gamma$	[Bar chart: 1σ to 2σ]				0.64	[Bar chart: 1σ to 2σ]				0.80
$e^- e^+ \nu_\mu \bar{\nu}_\mu \gamma$	[Bar chart: 1σ to 2σ]				0.86	[Bar chart: 1σ to 2σ]				1.30
$e^- e^+ \mu^- \mu^- \gamma$	[Bar chart: 1σ to 2σ]				0.59	[Bar chart: 1σ to 2σ]				1.03
$e^- e^+ e^- e^+ \gamma$	[Bar chart: 1σ to 2σ]				0.56	[Bar chart: -1σ to 2σ]				0.93
$e^- e^+ \nu_e \bar{\nu}_e \gamma$	[Bar chart: 1σ to 2σ]				0.65	[Bar chart: 1σ to 2σ]				0.83
$e^- \bar{\nu}_e u \bar{d} \gamma$	[Bar chart: 1σ to 2σ]				0.59	[Bar chart: 1σ to 2σ]				0.80
$\nu_e e^+ d \bar{u} \gamma$	[Bar chart: 1σ to 2σ]				0.60	[Bar chart: 1σ to 2σ]				0.72
$\nu_e \bar{\nu}_e u \bar{u} \gamma$	[Bar chart: 1σ to 2σ]				0.80	[Bar chart: 1σ to 2σ]				1.13
$\nu_e \bar{\nu}_e d \bar{d} \gamma$	[Bar chart: 1σ to 2σ]				0.73	[Bar chart: -1σ to 2σ]				1.10
$e^- e^+ u \bar{u} \gamma$	[Bar chart: -1σ to 2σ]				0.63	[Bar chart: -1σ to 2σ]				1.06
$e^- e^+ d \bar{d} \gamma$	[Bar chart: -1σ to 2σ]				0.77	[Bar chart: -1σ to 2σ]				1.25
$u \bar{d} s \bar{c} \gamma$	[Bar chart: 1σ to 2σ]				0.52	[Bar chart: 1σ to 2σ]				0.61
$u \bar{u} c \bar{c} \gamma$	[Bar chart: 1σ to 2σ]				0.68	[Bar chart: -1σ to 2σ]				1.26
$u \bar{u} s \bar{s} \gamma$	[Bar chart: 1σ to 2σ]				0.77	[Bar chart: 1σ to 2σ]				1.10
$d \bar{d} s \bar{s} \gamma$	[Bar chart: 1σ to 2σ]				0.73	[Bar chart: 1σ to 2σ]				0.96
$u \bar{u} u \bar{u} \gamma$	[Bar chart: 1σ to 2σ]				0.64	[Bar chart: -1σ to 2σ]				0.97
$d \bar{d} d \bar{d} \gamma$	[Bar chart: 1σ to 2σ]				0.67	[Bar chart: 1σ to 2σ]				0.84
$u \bar{u} d \bar{d} \gamma$	[Bar chart: 1σ to 2σ]				0.48	[Bar chart: 1σ to 2σ]				0.35

Integrated cross section

γ spectrum included, cuts applied



- W-pair threshold $\sqrt{s} \gtrsim 160$ GeV clearly visible
- γ spectrum reduces the cross section and shifts the threshold to higher energies
- Cross section decreases for high energies because of cuts

Remark: $\sigma_{\text{tot}}(\gamma\gamma \rightarrow WW) \rightarrow \text{const.}, \quad \sqrt{s} \rightarrow \infty.$

Comparison between different width schemes

$$\sigma(\gamma\gamma \rightarrow e^- \bar{\nu}_e \nu_\mu \mu^-)$$

$\sqrt{s_{\gamma\gamma}}$ [GeV]	500	800	1000	2000	10000
fixed width	826.40(21)	788.35(21)	746.94(21)	500.70(20)	31.745(68)
step width	827.45(22)	789.34(21)	748.17(23)	501.41(21)	31.746(68)
running width	827.43(23)	789.29(21)	748.11(23)	501.32(21)	31.715(68)
complex mass	826.23(21)	788.18(21)	746.78(21)	500.59(20)	31.738(68)

$$\sigma(\gamma\gamma \rightarrow e^- \bar{\nu}_e \nu_\mu \mu^- \gamma)$$

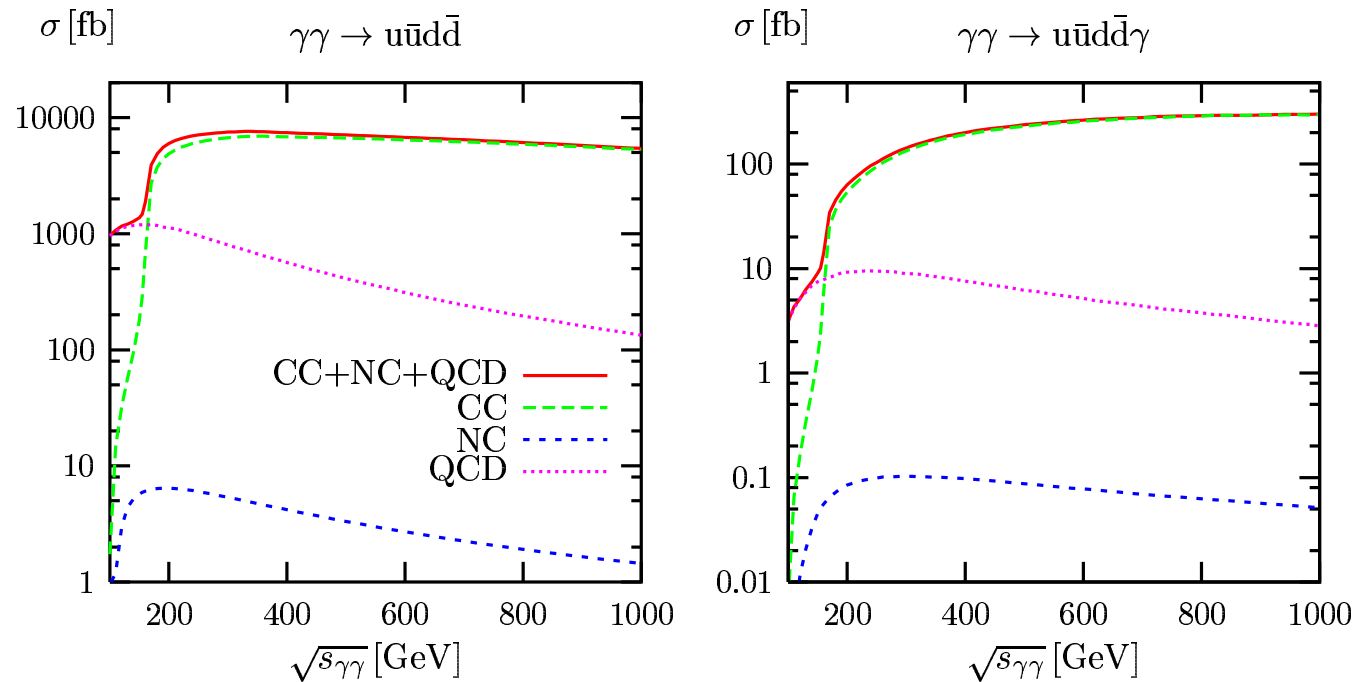
$\sqrt{s_{\gamma\gamma}}$ [GeV]	500	800	1000	2000	10000
fixed width	39.230(45)	47.740(73)	49.781(91)	43.98(18)	4.32(23)
step width	39.253(45)	47.781(73)	49.881(96)	44.01(18)	4.31(24)
running width	39.251(49)	47.781(74)	49.898(95)	44.48(22)	10.83(28)
complex mass	39.221(45)	47.730(73)	49.770(91)	43.97(18)	4.31(23)

⇒ Running width scheme yields **wrong** results from $\gamma\gamma \rightarrow 4f + \gamma$ at 1 TeV

⇒ Fixed width, step width, and **gauge-invariant complex-mass scheme** agree within $\mathcal{O}(\Gamma_W/M_W) \approx 2\%$.

Contributions to the cross section

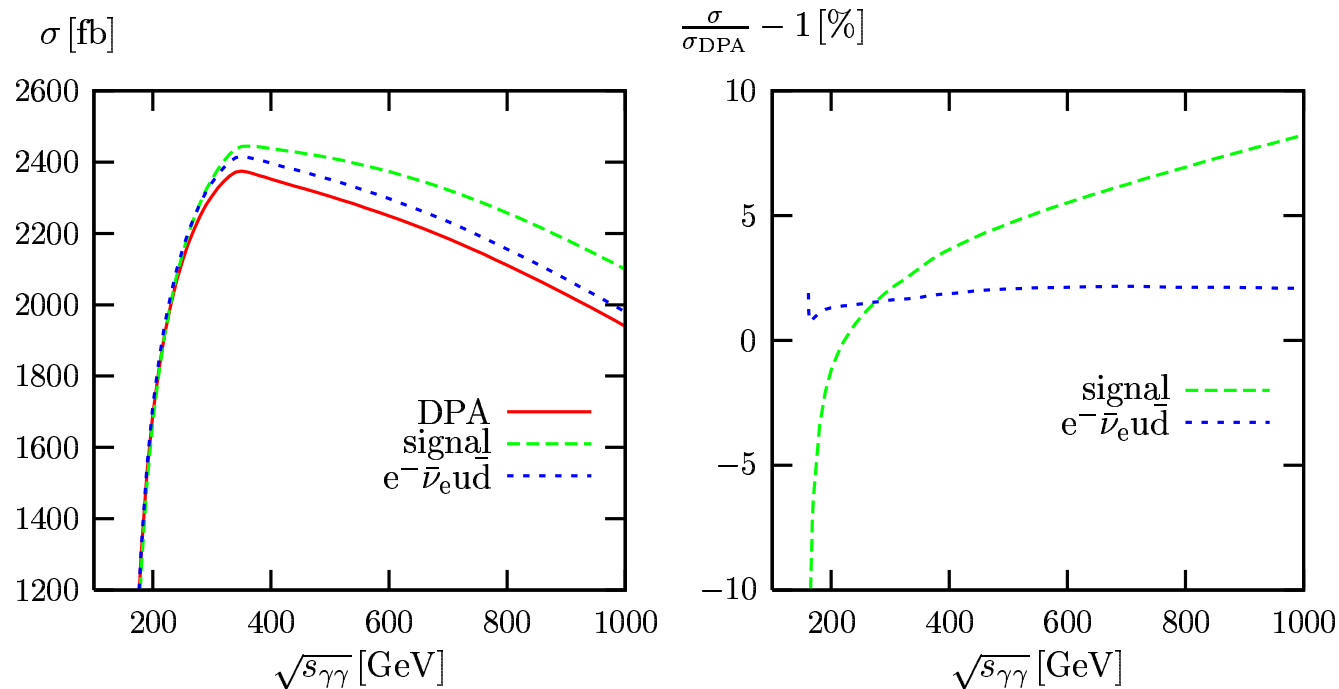
No γ spectrum included, cuts applied



- By far largest contribution from W -pair production (CC diagrams)
- Gluon-exchange contributions 1–2 orders of magnitude smaller
- NC diagrams negligible for CC processes

Signal diagrams versus double-pole approximation

No γ spectrum included, cuts applied



- Gauge-variant signal diagrams show large deviations of 5–10% for $\sqrt{s} = 0.5\text{--}1$ TeV
- Double-pole approximation (DPA) agrees within $\mathcal{O}(\Gamma_W/M_W) = 1\text{--}3\%$

⇒ Double-pole approximation is a promising approach to include radiative corrections into the theoretical predictions

Summary and outlook

Features of the calculation:

- Lowest-order prediction for **all** processes $\gamma\gamma \rightarrow 4f$ and $\gamma\gamma \rightarrow 4f + \gamma$ (including gluon-exchange diagrams)
- Monte Carlo generator **available** upon request
- **Photon beam spectrum** in the parametrization of COMPAZ implemented
- Non-standard **triple- and quartic-gauge-boson couplings** and an effective **$\gamma\gamma H$ coupling** can be optional included.

⇒ see talk of A. Bredenstein

Final aim of the calculation:

Calculation of the **$\mathcal{O}(\alpha)$ corrections in double-pole approximation** (similar to RACOONWW)